

20p.

N64-20817

CAT-24 code 1

Technical Memorandum No. 33-157

**Temperature Effect on Langmuir
Probe Measurement**

Che Jen Chen

NASA CN 56170

OTS PRICE

XEROX

\$ 1.60 ph

jpl

JET PROPULSION LABORATORY
CALIFORNIA INSTITUTE OF TECHNOLOGY
PASADENA, CALIFORNIA


October 30, 1963

508-16592

Technical Memorandum No. 33-157

*Temperature Effect on Langmuir
Probe Measurement*

Che Jen Chen



John Laufer, Chief
Fluid Physics Section

JET PROPULSION LABORATORY
CALIFORNIA INSTITUTE OF TECHNOLOGY
PASADENA, CALIFORNIA

October 30, 1963

**Copyright © 1963
Jet Propulsion Laboratory
California Institute of Technology**

**Prepared Under Contract No. NAS 7-100
National Aeronautics & Space Administration**

CONTENTS

I.	Introduction	1
II.	Measurements	2
III.	Calculations and Results	4
	A. Temperature Distribution Along the Probe	4
	B. Thermionic Emission Relation	5
	C. The Electric Field at the Surface of the Probe and Schottky's Effect	7
	D. The Voltage-Current (V - I) Characteristic Curves of the Probe	10
IV.	Discussion and Conclusions	12
	A. Effects on Diagnostic Results	12
	B. The Ratio of Ion and Electron Saturation Currents	13
	References	14

TABLES

1.	Work functions of the probe at different temperatures	10
----	---	----

FIGURES

1.	Schematic diagram of apparatus arrangement	3
2.	Probe temperature – electron emission characteristics	7
3.	Langmuir probe characteristics at different probe temperatures	11

ABSTRACT

20817

A

When a moderately heated tungsten Langmuir probe is immersed in an argon plasma in a discharge tube, a substantial lowering of its work function is observed. The mechanism is thought to be similar to the Schottky effect. The influence of this phenomenon on the accuracy of the probe measurements is discussed.

Author

I. INTRODUCTION

Since the early years of this century, the Langmuir probe has been used to measure the electron density, electron temperature, space potential, and other related phenomena in a plasma. The principle and operation of the probe are described in various periodicals and books (Ref. 1 and 2). The reliability of this instrument depends very much upon the conditions under which it is operated. Various possible sources of error in Langmuir probe techniques have been described previously by many authors (Ref. 3 and 4). For example, in Ref. 3 and 4 the authors conclude that the deposition of oxide on the surface of the probe causes the contact potential of the probe relative to the plasma to be changed; the work function of the probe is similarly changed. Also, when probing moderately high gas temperatures ($\sim 5000^\circ\text{K}$), the probe temperature may become sufficiently high and the electric field strength at the surface of the probe sufficiently large that the electron emission from the surface of the probe becomes considerably larger than that caused by simple thermionic emission alone. In the probe temperature range below 2000°K , thermionic emission is usually considered to be negligible. However, in the recent measurements described below, the characteristic curves of a hot Langmuir probe in a low density discharge tube revealed a saturation ion current at a probe temperature of 1900°K which was about one order of magnitude higher than that at room temperature. If this increase in ion current is interpreted as being caused by electron emission from the probe, the emission current is four orders of magnitude higher than the thermionic emission at the temperature concerned.

II. MEASUREMENTS

The apparatus arrangement is shown in Fig. 1. The discharge tubes are pyrex glass of various sizes (the typical dimensions are 15 cm in length, 2.5 cm in diameter). The electrodes are two tungsten disks 1.5 cm in diameter, 0.15 cm in thickness, and 12 cm apart. The probe is a 127- μ tungsten wire, 0.4 cm in length, which is demountable from the tube for replacement. The high-voltage power supply for the discharge is a regulated low ripple (25-mv peak-to-peak) source. The current through the probe is measured by determining the voltage drop across a standard resistance R_s . The current and voltage are recorded by a Moseley XY plotter which has a writing speed of about 2 in./sec on 15- by 10-in. graph paper. The dynamic accuracy is claimed to average 0.02%. The temperature of the probe is changed by varying resistance R_1 and is measured by an optical pyrometer with a 6500- \AA filter.

The temperature of the probe varies from point to point along the wire, but only the maximum temperatures at the midpoint of the probe are taken; the temperature distribution along the wire is then calculated as in the next Section. The temperatures recorded have been corrected for the emissivity of tungsten and the reflection of the glass surface. The electron temperature, electron density, and plasma potential are measured from the probe voltage-current characteristic curves. When the ion currents of the probe are measured at different temperatures, the voltage impressed on the probe is kept constant relative to one of the electrodes. This voltage is estimated to be high enough (negatively) for the probe to collect the saturation ion current.

The discharge voltage and current do not change when the probe temperature is increased.

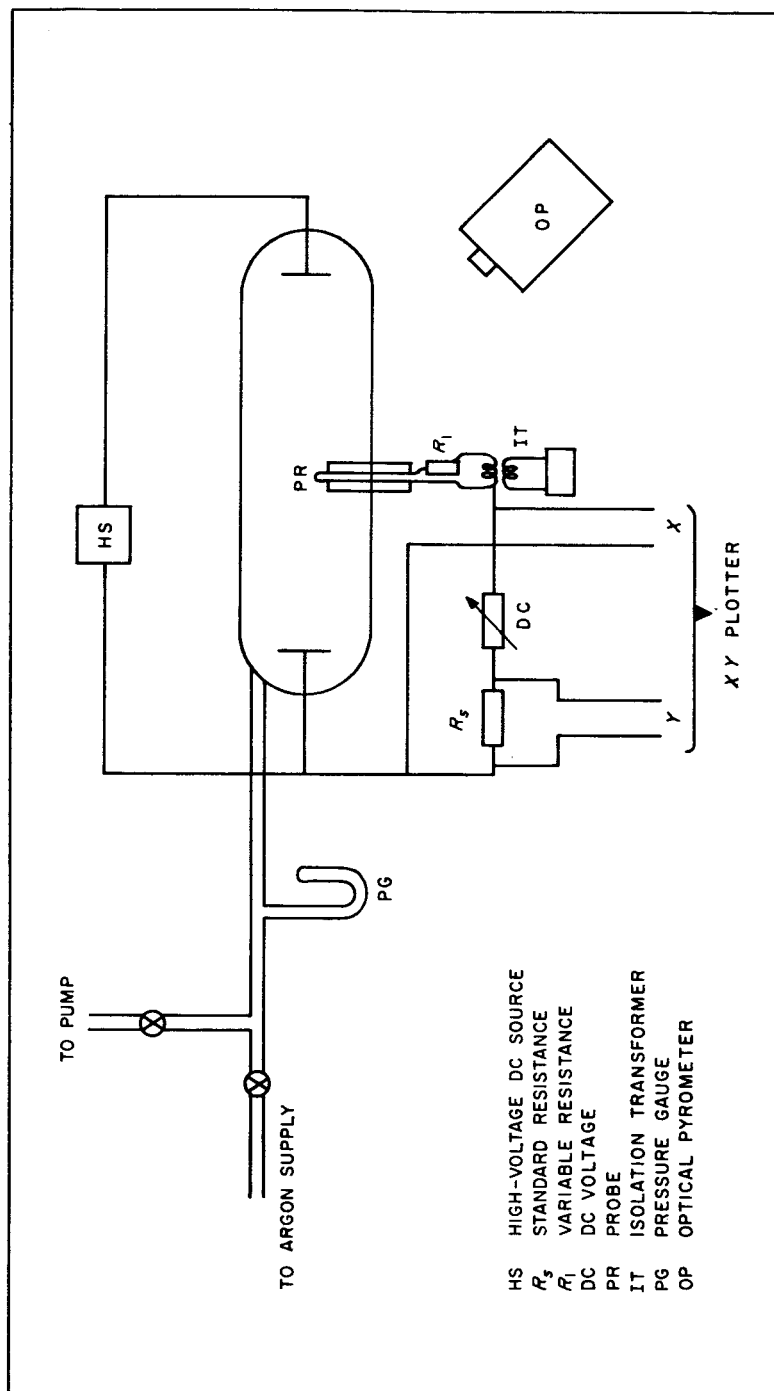


Fig. 1. Schematic diagram of apparatus arrangement

III. CALCULATIONS AND RESULTS

A. Temperature Distribution Along the Probe

Neglecting the radiation and convection losses ($\sim 0.01\%$ of conduction), the heat balance equation for an electrically heated wire of finite length has the following form (Ref. 5 and 6):

$$I^2 R_0 [1 + \alpha (T - T_0)] + A k \frac{d^2 T}{dx^2} = 0 \quad (1)$$

where

I = the heating current

R_0 = the resistance of the wire at temperature T_0 (in degrees Kelvin)

α = the temperature coefficient of resistivity of the wire

A = the cross-sectional area of the wire

k = the thermal conductivity of the wire

and

x = the distance along the wire from the midpoint

With the boundary conditions that

$$x = \frac{l}{2}$$

$$T = T_0$$

$$x = 0$$

$$\left\{ \begin{array}{l} T = T_m \text{ (maximum temperature)} \\ \frac{dT}{dx} = 0 \end{array} \right.$$

the solution of Eq. (1) can be written

$$T = a \cos \beta x + b \quad (2)$$

where

$$a = \frac{1}{\alpha} [1 + \alpha (T_m - T_0)]$$

$$b = T_0 - \frac{1}{\alpha}$$

$$\beta = \frac{2}{l} \cos^{-1} \left[\frac{1}{1 + \alpha (T_m - T_0)} \right]$$

l = length of the probe

B. Thermionic Emission Relation

The conventional expression for the thermionic emission is

$$j = c A' T^2 \exp \left(- \frac{e_1 \phi}{KT} \right) \quad (3)$$

where

j = current in amperes

c = constant

T = temperature of the probe

ϕ = work function in electron volts

A' = area of the probe in square centimeters

K = Boltzmann's constant

and

e_1 = electronic charge

Combining Eq. (2) and (3) and integrating over the whole length of the probe, we obtain the emission current i as the following expression:

$$i = 2 c A' \int_0^{l/2} (a \cos \beta x + b)^2 \exp \left(- \frac{e_1 \phi}{KT} \right) dx \quad (4)$$

For the tungsten probe,

$$\alpha = 0.010 \text{ for degrees centigrade}$$

$$c = 60.2 \text{ amp/cm}^2 \text{ for degrees centigrade}$$

$$l = 0.348 \text{ cm}$$

$$r = 6.35 \times 10^{-3} \text{ cm}$$

and

$$T_0 = 300^\circ\text{K}$$

Equation (4) is integrated numerically for different values of T_m and ϕ . The results are shown in Fig. 2.

In Fig. 2, the experimental data for three different discharge conditions are fitted to the curves of the suitable values of ϕ . The experimental values of i are obtained by subtracting the probe current at room temperature from that at probe maximum temperature T_m . The emission current i obtained in this way would be the current caused by electron emission from the surface of the probe, since the sign of this electron current is the same as the measured ion current.

It is interesting to note that the effective work function of the probe is lowered different amounts by the presence of plasma of different pressures and temperatures. This lowering of the work function might be caused by (1) the presence of electric and magnetic fields due to the heating current, (2) the effect of ion bombardment, and (3) the quasistatic electric field due to the plasma, etc. After estimating the order of magnitude of each effect, the most probable cause would seem to be the plasma quasistatic electric field. This will be discussed in the next Section.

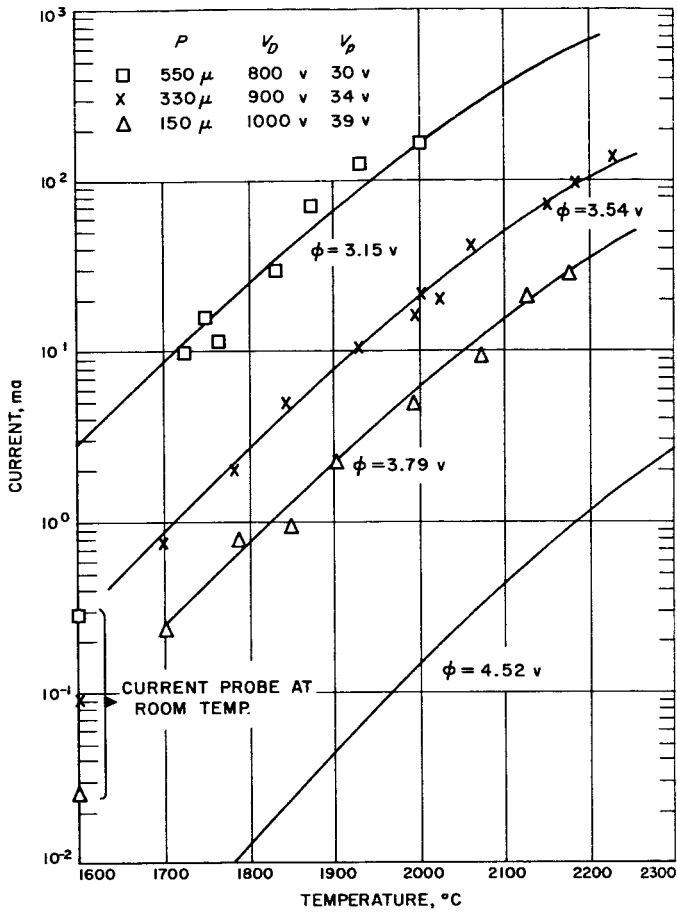


Fig. 2. Probe temperature - electron emission characteristics

C. The Electric Field at the Surface of the Probe and Schottky's Effect

Assuming that the electrons have a Maxwellian energy distribution, the equation describing the variation of electron density with potential V in the neighborhood of the probe can be written as

$$n_1 = n_0 \exp \left(- \frac{e_1 V}{KT_1} \right) \quad (5)$$

For a cylindrical probe the ion density, in the vicinity of the probe, can be expressed in the following form (Ref. 5, 6, and 7):

$$I_2 = \frac{n_0 e_2}{\pi} \left(- \frac{2e_2 V}{m_2} \right)^{1/2} 2\pi r \sin \frac{\pi n_2}{n_0} \quad (6)$$

where

n = charge number density

e = charge of the charged particle

I = electric current

m = mass

r = distance from the axis of the cylinder

T = temperature

and

K = Boltzmann's constant

The subscripts 1, 2, and 0 refer to the electron, ion, and undisturbed regions, respectively.

In deriving Eq. (6), we assume that the ions have reached energies which are large compared with their initial energies; the ionic velocity is equal to $(-2 e_2 V/m_2)^{1/2}$.

The distribution of potential in the vicinity of the probe is described by Poisson's equation:

$$\frac{1}{r} \frac{d}{dr} \left(r \frac{dV}{dr} \right) = -4 \pi (n_2 - n_1) e_2 \quad (7)$$

With Eq. (5) and (6), Eq. (7) can be solved numerically, considering I_2 as a parameter. However, if the dimension of the probe is large in comparison with the Debye length for the ion (as is the case in the present experiment), the plasma solution can give accurate results for the present discussion (Ref. 5 and 6). The fact that the electrons emitted from the surface of the negatively biased probe will counterbalance the excess positive space charges surrounding the probe could also justify the use of plasma solution.

For the plasma solution, by equating Eq. (5) and (6) and then differentiating V with respect to r , we obtain the expression for the electric field E :

$$E = \frac{dV}{dr} = \frac{2V}{\{\pi \eta \exp(-\eta) \cot[\pi \exp(-\eta)] - 1\} r} \quad (8)$$

where η stands for $(e_1 V/KT)$.

The effective lowering of the work function caused by the accelerating field, commonly referred to as Schottky's effect, has the following form (Ref. 8):

$$\phi_s = 3.79 \times 10^{-4} E^{1/2} \quad (9)$$

where

ϕ_s = lowering of the work function (in volts) caused by the accelerating field

and

E = electric field strength in volts/centimeter

Equations (8) and (9) yield

$$\phi_s = 3.79 \times 10^{-4} \left[2V / \{ \pi \eta \exp(-\eta) \cot [\pi \exp(-\eta)] - 1 \} r \right]^{1/2} \quad (10)$$

Using the results obtained from the probe voltage-current characteristic curves for three different operating conditions, the values of $\phi_{s(\text{calc})}$ are calculated by Eq. (10). Taking the work function for tungsten to be 4.52 ev, the values $\phi_{s(\text{meas})}$ are obtained from the experimental data as shown in Fig. 2. The calculated and experimental ϕ_s are compared in Table I, where

P = pressure of argon gas in the discharge tube

V_D = voltage impressed on the discharge tube

and

V_p = probe potential relative to the plasma

The measured plasma potential is affected by the temperature of the probe (see Section III-D). In Table I V_p is the probe potential relative to the plasma, with the plasma potential measured with the probe at room temperature. In spite of some approximations in the calculations, the calculated values $\phi_{s(\text{calc})}$ agree reasonably well with the measured values $\phi_{s(\text{meas})}$.

It is worthwhile to mention here that in the temperature range (1800 to 2500°C) and the field strength range (10^6 to 10^7 v/cm) of the present measurements, the electron emission has been classified as transition region emission and called *T-F* (temperature-field) emission (Ref. 9 and 10). The authors in Ref. 9 and 10 have provided experimental studies in which the theoretical expectations have been confirmed; however, the present data fit Schottky's theory better.

Table 1. Work functions of the probe at different temperatures

P, μ	V_D, v	$T_1, ^\circ K$	V_p, v	$\phi_{s(\text{calc})}, \text{ev}$	$\phi_{s(\text{meas})}, \text{ev}$
150	1000	4.56×10^5	39	0.504	0.73
330	900	3.97×10^5	34	0.618	0.98
550	800	3.50×10^5	30	1.56	1.37

D. The Voltage-Current (*V-I*) Characteristic Curves of the Probe

The *V-I* curves of the probe at different probe temperatures for the same operating conditions of the discharge tube are shown in Fig. 3. The following features are noticed:

1. The ion saturation current is increased as the temperature of the probe is increased. This is thought to be caused by electron emission from the surface of the probe of Schottky's type.
2. In general, as the temperature of the probe is increased, the electron saturation current remains almost unaltered, whereas the probe saturation current is lowered. This implies that the electron emission retains its original value as the probe voltage approaches the plasma potential. This phenomenon may be explained as follows: The thickness of the sheath surrounding the probe is decreased as the voltage of the probe relative to the plasma is reduced (Ref. 1 and 2). The field strength at the surface of the probe may remain almost constant. The electron emission remains the same so long as the probe temperature is the same.
3. The floating potential is increased as the temperature of the probe is increased. It can be shown theoretically that this change is in the right direction. If I_2 is the ion

saturation current, the floating potential V_f can be expressed approximately, by equating ion and electron currents, as follows:

$$V_f = \frac{KT_1}{e} \ln \frac{4 I_2}{A e n_1 c_1} \quad (11)$$

where

c_1 = the mean electron thermal speed

and

e = the absolute value of the electronic charge

Equation (11) indicates that V_f increases as I_2 is increased.

4. The plasma potential is decreased as the probe temperature is increased. This can be explained readily by noting that the electrons emitted from the probe make the plasma more negative in the vicinity of the probe.

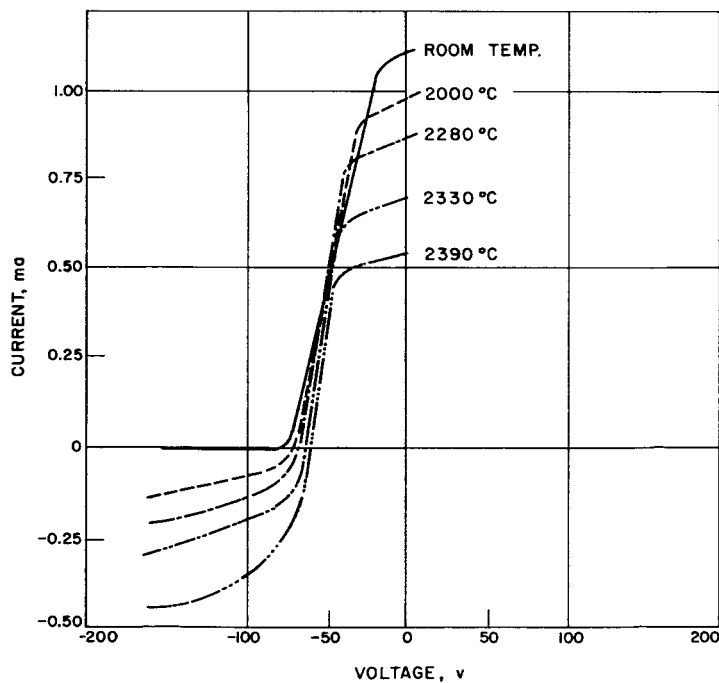


Fig. 3. Langmuir probe characteristics at different probe temperatures

IV. DISCUSSION AND CONCLUSIONS

A. Effects on Diagnostic Results

If the temperature of the probe is high enough, as indicated in the previous Sections, the following possible effects on the diagnostic results may be anticipated:

1. Electron temperature measurement by slope of the $V-I$ curve: Since the floating potential is increased and the plasma potential is decreased as the temperature of the probe increases, the slope of the $V-I$ curve in the region of slightly negative voltage becomes steeper with increasing probe temperature. The measured electron temperature thus appears to be lower than the expected value. As indicated in Fig. 3, for this particular run the electron temperature appears to be lowered about 30% as the temperature of the probe goes from room temperature to 2000°C.
2. Electron density measurement by electron saturation current: Since the electron saturation current is not altered appreciably by the probe temperature, the electron density is only affected by the uncertainty of electron temperature measurement. In the formulas used for electron density calculations (Ref. 1 and 2), a factor of $(1/T_e^{1/2})$ is involved. Therefore, in the particular case described above, the electron density appears to be higher by about 15%.
3. Ion density measurement by saturation current: It can be seen from Fig. 2 and 3 that the probe temperature has a most serious effect on this parameter. Again, referring to the case mentioned above, the ion saturation current at 2000°C is more than one order of magnitude higher than that at room temperature; so will be the ion density calculated therefrom.
4. The effects on floating potential and plasma potential measurement: In this particular case, the floating potential increases about 5 v and the plasma potential decreases 4 v.

B. The Ratio of Ion and Electron Saturation Currents

The ratio I_1/I_2 has the form (Ref. 5 and 6)

$$\frac{I_1}{I_2} = \left(\frac{m_2}{m_1} \right)^{1/2}$$

where

m_1 = the mass of the electron

and

m_2 = the mass of the ion

For argon,

$$\frac{I_1}{I_2} \sim 270$$

Many observers (Ref. 11 and 12) have previously found that the values of I_1/I_2 for argon or other gases in arc-heated plasma-jet measurements are almost one order of magnitude less than the expected ones. This discrepancy is thought to be caused by electron attachment on neutral atoms to form negative ions, thus increasing the effective mass of the negatively charged particles. However, experimental measurements (Ref. 13) indicate that argon gas does not form negative ions. The electron emission from the surface of the probe observed in the present experiments may account (wholly or partially) for such a discrepancy in the ion-electron saturation current ratio.

REFERENCES

1. Langmuir, I., and Mott-Smith, H., "Studies of Electric Discharges in Gases at Low Pressures," *General Electric Review*, Vol. 27, 1924; Part I, pp. 449-455; Part II, pp. 538-548; Part III, pp. 616-623; Part IV, pp. 762-771; Part V, pp. 810-820.
2. Loeb, L. B., *Basic Processes of Gaseous Electronics*, University of California Press, Berkeley, California, 1961, pp. 329-370.
3. Easley, M. A., "Probe Technique for the Measurement of Electron Temperature," *Journal of Applied Physics*, Vol. 22, 1951, p. 590.
4. Wehner, G., and Medicus, G., "Reliability of Probe Measurements in Hot Cathode Gas Diodes," *Journal of Applied Physics*, Vol. 23, 1952, p. 1035.
5. Ladenburg, R. W., *Physical Measurements in Gas Dynamics and Combustion*, Princeton University Press, Princeton, New Jersey, 1954.
6. Allen, J. E., Boyd, R.L.F., and Reynolds, P., "The Collection of Positive Ions by a Probe Immersed in a Plasma," *Proceedings of the Physical Society* (London), Vol. 70, Part 3-B, 1957, pp. 297-304.
7. Bohm, D., Burhop, E.H.S., and Massey, H.S.W., *The Characteristics of Electrical Discharge in Magnetic Field*, ed. by A. Guthrie, McGraw-Hill Book Co., Inc., New York, 1949.
8. Van Der Ziel, Albert, *Solid State Physical Electronics*, Prentice-Hall, Inc., Englewood Cliffs, New Jersey, 1957, pp. 105-118.
9. Dolan, W. W., and Dyke, W. P., "Temperature and Field Emission of Electrons from Metal," *The Physical Review*, Vol. 95, 1954, p. 327.
10. Dyke, W. P., et al., "T-F Emission: Experimental Measurement of the Average Electron Current Density from Tungsten," *The Physical Review*, Vol. 99, 1955, p. 1192.
11. Jahn, R. G., and Von Jaskowsky, W., *Langmuir Probe Measurement in Plasma Jet*, Plasmadyne Report No. PLR-34, Plasmadyne Corp., Santa Ana, California, 1959.
12. Clayden, W. A., *Rarefied Gas Dynamics*, ed. by L. Talbot, Academic Press Inc., New York, 1961, p. 715.

REFERENCES (Cont'd)

13. Bates, D. R., "The Study of Negative Ions by Extrapolation Through Isoelectronic Series,"
Proceedings of the Royal Irish Academy, Vol. A51, 1947, p. 153.